PRECEDING PAGE BLANK NOT FILMED N/S

N94-24305

S2-91 170682 p-4

WHOLE ROCK MAJOR ELEMENT CHEMISTRY OF KREEP BASALT CLASTS IN LUNAR BRECCIA 15205: IMPLICATIONS FOR THE PETROGENESIS OF VOLCANIC KREEP BASALTS.

Scott K. Vetter, Department of Geology, Centenary College, Shreveport,LA, 71104 and John W. Shervais, Department of Geological Sciences, University of South Carolina, Columbia, SC, 29208.

KREEP basalts are a major component of soils and regolith at the Apollo 15 site. Their origin is controversial: both endogenous (volcanic) and exogenous (impact melt) processes have been proposed, but it is now generally agreed that KREEP basalts are volcanic rocks derived from the nearby Apennine Bench formation [1-5]. Because most pristine KREEP basalts are found only as small clasts in polymict lunar breccias, reliable chemical data are scarce [5-8]. The primary aim of this study is to characterize the range in chemical composition of pristine KREEP basalt, and to use these data to decipher the petrogenesis of these unique volcanic rocks.

Lunar breccia 15205 is a polymict regolith breccia that consists of approximately 20% KREEP basalt clasts and 20% quartz-normative basalt clasts in a KREEP-rich matrix [9]. The clasts range up to 1 cm in size, but most are considerably smaller. Seventeen fragments of pristine KREEP basalt were extracted from the remaining large subsamples of 15205, however, due to their small size (< 5mm), only 13 were large enough for whole rock analysis. These clasts were analyzed for trace element geochemistry by INAA [7]. After the irradiated samples were cool enough to ship, they were transferred to the University of South Carolina for fused bead electron microprobe analysis (EMPA). The samples were removed from their silica glass tubes, powdered, and fused in Mo foil boats prior to analysis for 12 major and minor elements on a Cameca SX-50 electron microprobe. Eight clasts (including 3 too small for whole rock analysis) were prepared as polished probe mounts for petrographic examination and mineral analysis.

PETROGRAPHY AND MINERAL CHEMISTRY: 15205 KREEP basalt clasts are characterized petrographically by 45-50 vol% plagioclase, 40-50 vol% pyroxene, and mesostasis. Most are medium to coarse-grained basalts with textures grading from ophitic or subophitic to intersertial within the same rock. The irregularly distributed mesostasis consists of K-rich glass, K-feldspar, silica, Ca-phosphate, and ilmenite. Ilmenite occurs as discrete slender grains between the coarser silicate phases; other mesostasis phases form granular patches. Plagioclase ranges in composition from An78 to An88. Pyroxene have pale tan magnesian pigeonite cores (En76 Wo4 to En67 Wo5) with rims of greenish ferroan pigeonite or augite pyroxene (En42 Wo15 - En33 Wo39). One clast has a fine-grained, variolitic texture consisting of quenched pyroxene (En69 Wo5 - En49 Wo25) with an opaque glass and ilmenite between the varioles.

WHOLE ROCK GEOCHEMISTRY: The major element data presented here show that KREEP basalt clasts from 15205 span a limited range in composition compared to earlier studies [e.g, Irving, 1], but are essentially identical in compositional range to the KREEP basalts analyzed by Ryder [6]. Calculated Mg#'s range from 53 to 66 (MgO = 6.4 to 11.3 wt%) (Table 1). SiO_2, TiO_2, K_2, and P_2O_5 all increase with decreasing MgO, whereas FeO, CaO, and Al_2O_3 show little or no change throughout the range of MgO contents (Figure 1). Based on these relationships, a parent liquid can be postulated similar in composition to 15205 ,140 from which the other samples may be derived by fractional crystallization (sample ,158 is more primitive, but appears not to represent a liquid composition). Deviations from pure fractional crystallization trends may be caused by non-representative sampling of the small, coarse-grained clasts [e.g., 7]. This view is supported by the trace element data [7], which show little or no correlation with major element fractionation indices. Lindstrom et al. [7] have suggested that the observed scattering in trace elements concentrations could result from small variations in mesostasis distribution, and that all of these samples may come from a single flow. This interpreatation (dervied from a single lava flow) is at odds with the observed major element variations, which are similar to those seen in terrestrial magma suites.

DISCUSSION: Fractional crystallization models can be tested using least squares mixing models with an assumed or calculated parent magma composition and observed or hypothetical liquidus phases. Calculations take the form parent = daughter + liquidus phases, and reasonable solutions are assumed to have squared residual sums < 1.0. Calculations using ,140 as the assumed parent magma and the observed liquidus phases (Opx, Plag) fail to obtain good fits (r^2 = 3). Good fits are obtained when olivine is added to the fractionating assemblage (r^2 = 0.7 to 0.9), with 72% total fractionation required to obtain the most evolved compositions (38% plag, 27% opx, 7% olivine). Plagioclase dominates the fractionating assemblage, in keeping with the high alumina content of KREEP basalts. A problem with these solutions is that olivine in not observed as phenocrysts in KREEP basalts, nor do they appear to be olivine saturated in a silica-olivine-plagioclase ternary plot [e.g., 5]. The lack of modal olivine may be due to resorption of early formed olivine during slow cooling.

CONCLUSIONS: KREEP basalt clasts from breccia 15205 appear to represent a fractionation series related to a common parent magma. The range in major element compositions is too large to form by non-representative sampling of a single flow, but the lack of correlation between major elements and trace elements suggests that mesostasis distribution in these coarse-grained samples does not represent magmatic compositions.

Table 1. Whole rock geochemistry of KREEP basalt clasts in 15205

	,146	,131	132	,142b	,163	,135	,148	,161B	,133	,165	,167	,158	,140
SiO2	51.27	50.34	51.25	51.83	50.04	51.03	50.78	50.66	50.96	52.88	50.15	48.34	49.75
TiO2	2.07	1.99	1.92	1.78	2.36	2.07	2.20	2.03	2.41	2.13	1.94	2.02	1.40
Al2O3	16.09	15.38	16.28	18.33	14.61	15.78	15.67	16.98	16.81	15.38	15.92	15.37	16.90
FeO	10.17	10.71	9.79	9.31	11.52	10.15	10.23	9.85	9.97	10.11	10.33	10.80	9.65
MnO	0.16	0.16	0.15	0.11	0.18	0.12	0.15	0.18	0.14	0.14	0.15	0.16	0.14
MgO	7.33	8.81	8.49	8.79	8.19	8.85	8.53	8.27	8.41	7.18	9.32	11.31	10.45
CaO	10.31	10.11	10.10	10.06	10.16	9.97	10.14	10.58	10.23	9.70	9.99	9.43	9.67
Na2O	0.87	0.81	0.84	0.78	0.81	0.81	0.82	0.79	0.82	0.91	0.76	0.72	0.78
K2O	0.67	0.54	0.58	0.55	0.65	0.56	0.54	0.37	0.67	0.83	0.49	0.34	0.40
P2O5	0.35	0.29	0.22	0.23	0.54	0.29	0.41	0.16	0.47	0.44	0.30	0.23	0.11
Cr2O3	0.27	0.34	0.32	0.31	0.29	0.31	0.32	0.31	0.26	0.28	0.33	0.43	0.36
Sum	99.56	99.48	99.92	100.08	99.36	99.94	99.95	100.18	99.16	99.98	99.68	99.15	99.60
Mg#	56.22	59.46	60.74	62.71	55.90	60.85	59.77	59.94	53.43	55.86	61.67	65.11	65.87

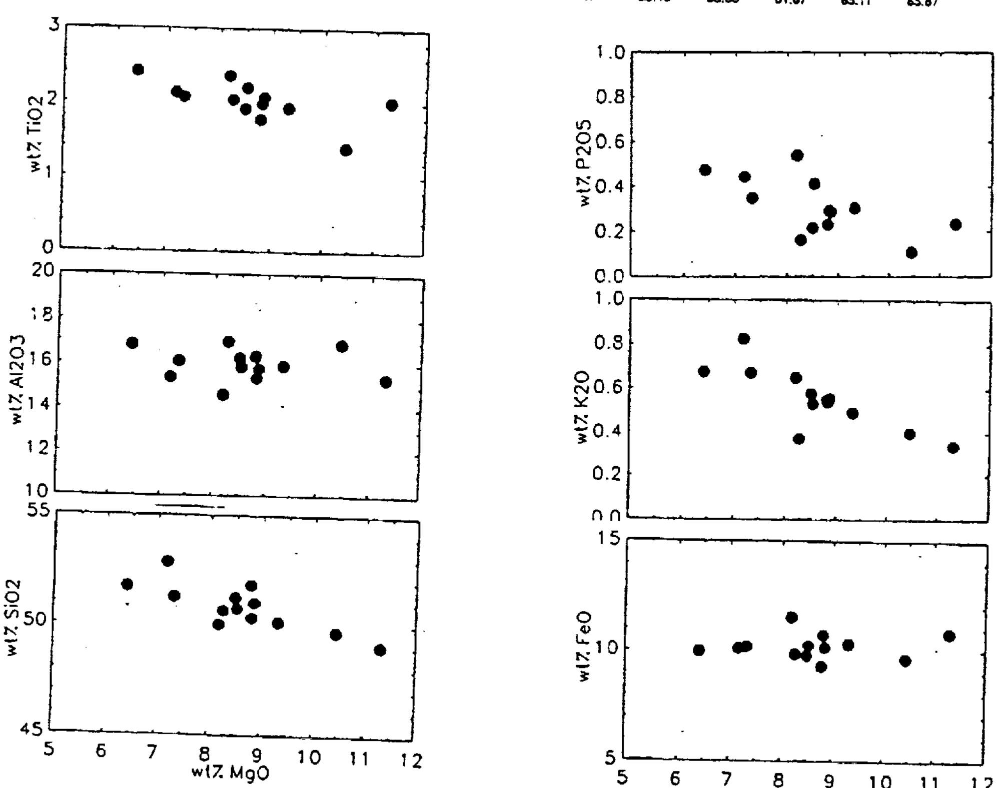

Figure 1. MgO-variation diagrams for KREEP basalt clasts from lunar breccia 15205.

REFERENCES: [1] Irving (1977) PLSC 8th, 2433. [2] Spudis and Hawke (1986) LPI Tech. Rpt. 86-03, 105. [3] Dymek (1986) LPI Tech. Rpt. 86-03, 52. [4] Ryder (1987) PLSC 17th, E331. [5] Ryder (1989) LPSC XX, 936. [6] Shervais and Vetter (1989) LPSC XX, 1000. [7] Lindstrom et al. (1989) LPSC XX, 578. [8] Ryder (1988) LPSC XIX, 1011. [9] Dymek et al. (1974) PLPSC 5th, 235-260. [10] Shervais et al. (1990) PLPSC 20th, 109-126.